The evolution of Chabahar beach ridge system in SE Iran in response to Holocene relative sea level changes

Majid Shah-Hosseini [a,b,*], Ezatollah Ghanavati [a], Christophe Morhange [b], Abdolmajid Naderi Beni [c], Hamid Alizadeh Lahijani [c], Mohammad Ali Hamzeh [c]

[a] Kharazmi University, Geomorphology Department, Moffateh St., Tehran, Iran
[b] Aix-Marseille Université, CNRS, IRD, CEREGE UM34, 13545 Aix en Provence, France
[c] Iranian National Institute for Oceanography and Atmospheric Science (INIOAS), 3 Etemadzadeh St, Fatemi Av., Tehran, Iran

ABSTRACT

The Chabahar Strandplain (CHS) stretches along the Chabahar bay at a width of more than 5 km along the northern coast of the Gulf of Oman and SE Iran; an area that has been subjected to tectonic uplift as a part of the Makran accretionary prism. The CHS comprises of beach ridges, inter-ridge swales, sand dunes, tidal channels and fluvial deposits. We present the first documentation of the spatial distribution and the internal architecture of the CHS based on topographic surveys, sediment percussive coring, trenching and ground penetrating radar (GPR) transects. Radiocarbon dating on marine shells from foreshore deposits of 8 representative beach ridges yielded ages between 4800 and 270 cal. years BP at respective distances of 4800 to 670 m from the present shoreline. We interpret the boundary between the foreshore (beach) and the foredune deposits as indicator of past sea levels by analogy to present shore processes. This boundary is readily recognizable in sediment profiles from cores and trenches as well as GPR reflectors. Based on the age model and depositional features, we estimate relative sea level fall of up to 15 m over the past 4800 years. Considering that the eustatic sea level changes for this period are negligible for the Makran coast, this relative sea level fall is related to tectonic uplift across the coastal Makran. The elevation of palaeo-shorelines with similar ages decrease from east to west of the CHS, which suggest that alongshore variations in uplift rates are likely related to different movements of coastal fault blocks.

© 2017 Elsevier B.V. All rights reserved.

1. Introduction

The low-relief coastal areas of the world are under ongoing threat of sea level rise (Church et al., 2013). The knowledge of past relative sea level changes is essential for understanding coastal evolution and trends of future sea level changes. Beach ridges are among common landforms in prograding coasts and have the potential to provide high-resolution records of coastal processes, the position of former shoreline and relative sea level changes (Otvos, 2000; Goy et al., 2003; Anthony, 2009; Tamura, 2012).

A beach ridge is defined as a relict, elongate body of sand or gravel-sized sediment that stretches parallel or semi-parallel to the shoreline (Otvos, 2000). A strandplain, also referred to as beach-ridge system, corresponds to a coastal plain characterized by a series of beach ridges separated by shallow swales. It consists of surficial and subsurface sediments and structures with a worldwide distribution across all latitudes and continents (Scheffers et al., 2012). Understanding the internal

architecture of strandplain is essential for interpretation of the origin, formational processes and the position of former shorelines.

Holocene strandplains have been studied in many coastal environments including those in Australia (Bristow and Pucillo, 2006; Oliver et al., 2017), New Zealand (McSaveney et al., 2006) north America (Moore et al., 2004; Billy et al., 2014, 2015), South America (Hesp et al., 2005), Northern Europe (Brückner and Schellmann, 2003; Clemmensen and Nielsen, 2010), Southern Europe (Goy et al., 2003), west Africa (Anthony, 1995) and eastern coast of Japan (Tamura et al., 2008, 2010; Tamura, 2012). Most studies have focused on reconstruction of past relative sea level changes based on strandplain deposits (Searle and Woods, 1986; Tanner, 1988; Thompson, 1992; Thompson and Baedke, 1995; Blum et al., 2003; Rodriguez and Meyer, 2006; Tamura et al., 2008; Clemmensen and Nielsen, 2010). The application of geophysical subsurface profiling techniques, in particular, along with topographic and sedimentological studies are of great importance in integrated studies of strandplains. Ground-penetrating radar (GPR) techniques have been especially found useful in recent beach ridge studies (Van Heteren et al., 2000; Jol et al., 2002; Nott et al., 2009; Clemmensen and Nielsen, 2010; Tamura et al., 2008, 2010, 2017; Billy et al., 2014; Oliver et al., 2017).
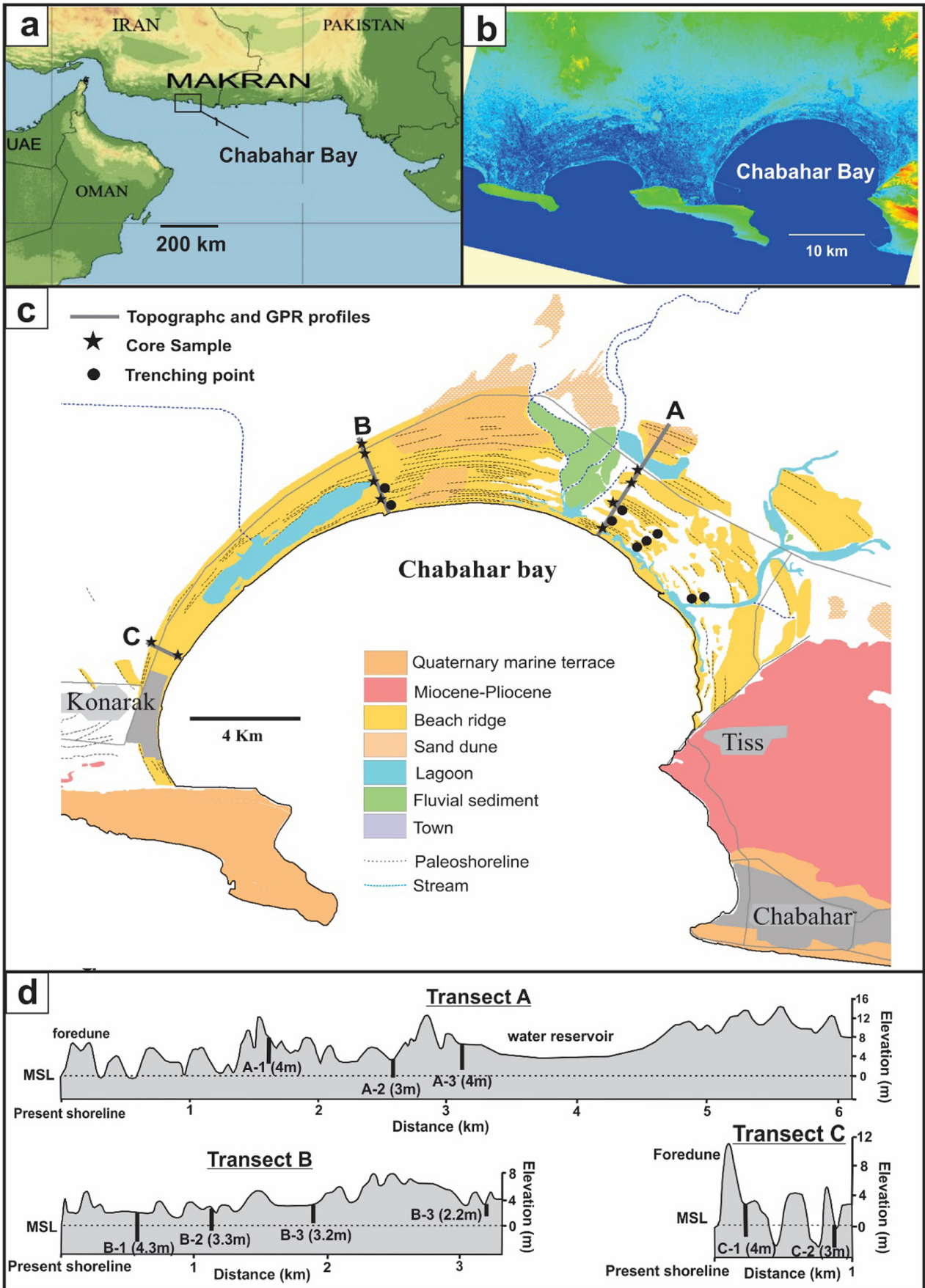
Fig. 1. (a) Location map of the study area. (b) Spot-DEM digital elevation model of Chabahar bay and adjacent area. (c) Geomorphologic map of the Chabahar strandplain with position of three coastal transect and sediment sampling sites. (d) Topographic profile of three studied transects with position of collected sediment cores.

The development of strandplains is a common feature in uplifting coasts. Intensive beach ridge systems have been studied in details in uplifting coasts such as eastern Japan (Tamura et al., 2008, 2010) and New Zealand (McSaveney et al., 2006). The presence of relict shorelines in the coast of Makran in SE Iran was reported in pioneering geographical and geological reports (Snead, 1970; Page et al., 1979). In the coast of Makran, strandplains are developed around semi-circular headland protected embayments. In more recent paleogeographical studies, paleoshorelines around Chabahar Bay were described and their age was estimated by radiocarbon dating on marine shells. (Gharibreza and Motamed, 2006; Gharibreza, 2016). In the current study, we investigate a well-developed strandplain around Chabahar Bay in the central part of the Iranian coast of Makran. We document the internal architecture of the strandplain for the first time. By combining high-resolution spatial data from satellite images, Digital Elevation Models (DEMs) and field surveys with GPR subsurface profiles and sediment cores, we further aims to determine the origin and chronological evolution of the Chabahar strandplain. Finally, we use radiocarbon dating in conjunction with spatial positioning of former shores to reconstruct relative sea level changes since mid-Holocene.

2. Study area

2.1. Geological setting

Chabahar Bay is located on the Iranian coast of the Makran, on the northern flank of the Gulf of Oman in north-western Indian Ocean (Fig. 1a). The coast is part of the Makran accretionary wedge, formed by subduction of the Arabian plate under the Eurasian plate (Byrne et al., 1992; Regard et al., 2005). The convergence rate along the Makran subduction zone varies between 2.3 cm/y to the west and 2.9 cm/y on the eastern parts of the accretionary wedge (Regard et al., 2005). The uplift rate during the Holocene is estimated to range between 0.1 and 0.6 m/ka in various parts of the coast (Page et al., 1979; Reyss et al., 1998; Prins et al., 2000).The coast of Makran is marked by a series of prominent headlands and embayments with Chabahar Bay in the middle section of the coast. The interior shore of the bay consists mainly of sandy and gravelly beaches. The bay is partially protected from ocean swells and storms by uplifted rocky headlands at the opening (Page et al., 1979; Reyss et al., 1998). Relict beaches and foredune ridges separated by inter-ridge swells, lagoons and tidal channels form a wide strandplain that stretches about 35 km along and more than 5 km across the shore. The strandplain is confined to the east by a fault in the upper Miocene-Pliocene marls and sandstones, and by Pleistocene marine terraces to the west (McCall et al., 1985) (Fig. 1c). Active and abandoned tidal channels that connect to raised lagoons stretch across the strandplain. In the western part of the bay a raised lagoon separates the beach ridges and relict foredunes. The lagoon is connected to the sea *via* a narrow channel and gets inundated during storms intermittently. In the eastern side of the bay, a portion of an abandoned lagoon is modified with earth walls to collect flood water for agriculture. Scarce seasonal streams pass through marl and sandstone formations flow through the strandplain and drain to the Chabahar Bay forming wadies connected to the tidal channel systems (Fig. 1c).

2.2. Wave climate and land use

The coast is wave-dominated and mesotidal. The diurnal tidal oscillations in Chabahar bay varies between −2 and +2.8 m relative to the local geoid. The maximum spring tidal range is 3 m. The strongest waves appear in January to June in accordance with south-eastern summer monsoon. The significant wave height reaches 3 m (Hydrological Department of the National Cartographic Center of Iran). Urban settlement, industrial infrastructures and agriculture were very limited on Chabahar strandplain at the time of this study (2012).

3. Field and analytical methodology

3.1. Mapping and topographic survey

In the course of three field campaigns from 2009 to 2012, topographic profiles, GPR data and sedimentary cores were collected along three representative shore-normal transects around the Chabahar Bay. A detailed geomorphologic map of Chabahar strandplain was prepared based on high-resolution SPOT-5 satellite images (1 pixel = 2.5 m) and satellite radar Digital Elevation Model (SPOT-DEM) (Fig. 1b; c).

The mapping process was complemented by direct investigations and ground-truthing in the field. Coordination and elevation of coastal profiles were recorded by point-to-point method using a differential GPS system (Fig. 1d). The reference for elevation was the local geoid (WGS84), which was assumed as the mean sea level. Although the vertical accuracy of the measurements is theoretically 10 cm, we assumed a more conservative value of 50 cm to account for poor signal quality. The measurements were checked by replicate occupation of one survey profile. A detailed gomorphological map of the study area was developed by processing the spatial data in MapInfo version 8 (Fig. 1c; d).

3.2. Ground penetrating radar (GPR) profiles

More than ten kilometers of subsurface profiles were collected along three shore-normal transacts (Fig. 1c). A MALA Geo-Science GPR system with a 100-MHz, unshielded transmitter was used during this study. The GPR system transmits and collects radar signals to the maximum depth of 10 m with vertical resolution of 0.2 m. However, presence of brackish groundwater reduces the effective radar penetration depth to about 6 m for most collected profiles. In order to add the topography of the surface to GPR profiles, topographic data were collected simultaneously using a DGPS set coupled with GPR system. Reflex 2DQuick software was used for standard data processing and corrections.

3.3. Core sampling and sediment analysis

The sedimentology of the Chabahar Bay strandplain was investigated using data from sediment cores, open trenches and natural outcrops (Fig. 1c). Nine sediment cores ranging from 2 to 6 m were collected using a percussive corer powered by an eight horsepower Cobra TT gas motor hammer. A set of open-side steel tubes with the opening widths of 6 to 10 cm were used for sediment recovery. Each core was logged and systematically sub-sampled in the field. A Total of 12 trenches were excavated for direct sedimentological study. All excavated trenches were oriented perpendicular to the trend of the ridge's crest. Sediment samples were collected from trenches and natural outcrops. The particle size distribution was measured in sediment samples using standard sieve series for sand and gravel fractions and by laser diffraction granulometry for silt and clay fractions. The carbonate and organic matter content were measured by standard loss-on-ignition method. A binocular microscope was used to determine roundness, sorting and lithology of sediment samples.

3.4. Age determination

Considering the abundance of marine shells in beach ridge deposits, radiocarbon dating method was chosen to determine the age of Chabahar strandplain. Mollusk samples collected *in situ* from trenches and outcrops were preferred for dating due to lower risk of displacement and depth uncertainties. The chronology presented here mainly relies on radiocarbon dating of eight marine shells collected from foreshore deposits of the beach ridges along transect A in the eastern part of Chabahar Bay strandplain (Fig. 5; Table 3). Pristine marine mollusk shells were sent to Poznan radiocarbon laboratory. The radiocarbon dates were calibrated and corrected using marine 13.14C calibration curve (Reimer et al., 2013). A marine reservoir age correction
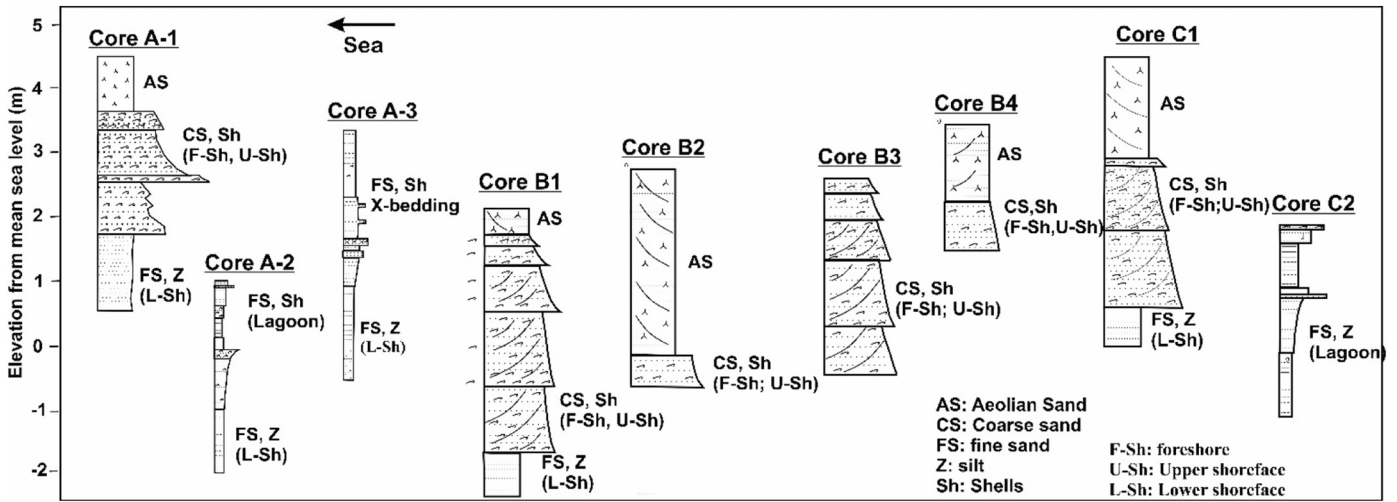
Fig. 2. Sedimentary profile of core samples from transect A, B and C.

of ΔR = 190 ± 25 years for the Arabian Sea and the gulf of Oman (Southon et al., 2002) was applied to the final calibrated radiocarbon ages.

4. Results

4.1. Spatial distribution of Chabahar Bay strandplain

The topography and spatial distribution of landforms considerably vary in the Chabahar Bay strandplain. In the eastern part (Transect A), the width and height of the strandplain are at their maximum (Fig.1c). An active foredune is developed along the shore and the strandplain in this section consists of series of prominent relict foredunes separated by raised tidal channels and lagoons. At least 14 distinct relict foredune crests were identified in the field and on satellite images (Fig.1c). A gradual landward increase in the elevation of the beach ridge crests is documented in topographic profiles (Fig. 1d). In the landward extreme of the strandplain, foreshore (beach) deposits are found about 5400 m inland from the active shoreline and more than 15 m higher than the mean sea level. In transect A, three sediment cores 3–4 m long were successfully recovered (Fig. 2). Further attempts for coring were unsuccessful due to consolidated sediments or the presence
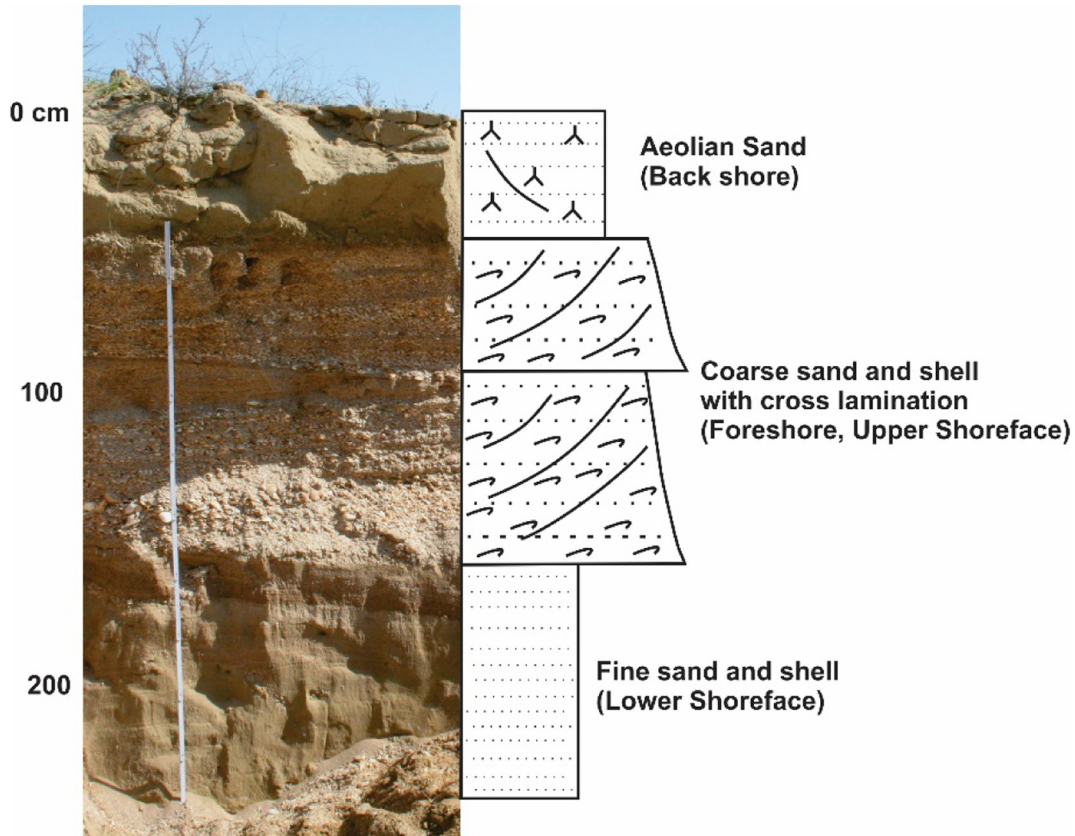

Fig. 3. Sedimentary profile of beach ridge sequence in a cross-cutting trench.

Table 1
Carbonate content and grain size analysis for sediment samples from modern shoreline and Chabahar strandplain.

Sample name	Setting	CaCO₃%	Grain Size		
			Sand%	Silt%	Clay%
Ch 1	Modern foreshore	69	94	6	0
Ch 2	Modern foreshore	79	97	4	0
Ch 3	Modern foreshore	70	95	5	0
Ch4	Modern upper shoreface	68	91	7	2
Ch5	Modern lower shoreface	30	70	25	5
Unit 1	Aeolian sand	39	63	37	0
Unit 2	Relict foreshore	71	94	6	0
Unit 3	Relict shoreface	37	73	24	3

of compact shell layers. The sedimentary profile of beach ridges was documented through natural outcrops and excavated trenches.

The middle segment of the strandplain along transect B is approximately 3400 m wide (Fig. 1c; d). It consists of a series of successive shore-parallel relict ridges, partially covered by longitudinal aeolian dunes. Sand dunes are mainly aligned to the direction of prevailing winter monsoonal winds (southwest-northeast). In the middle section, relict foreshore sediments are found to a maximum elevation of 8 m from mean sea level. Four percussive sediment cores were successfully collected along transect B (Fig. 2).

Transect C is located on the westernmost part of the Chabahar Bay strandplain near the fishery port of Konarak (Fig. 1c). This transect covers the narrowest and lowest part of Chabahar strandplain. To the southwest, the strandplain is terminated to Pleistocene marine terraces (Fig. 1c). Geomorphic landforms are limited to a prominent modern foredune and two distinct beach ridges separated by a raised back-barrier lagoon. The crest of the active foredune is up to 12 m higher than the mean sea level. Two percussive cores were successfully collected in this section (Fig. 2). Foreshore sediments were found under capping aeolian sand to a distance of 0.9 km and elevation of about 2 m above the mean sea level.

4.2. Sedimentology of beach ridge deposits

In all transects (Fig. 1c), a complete sequence of beach ridge deposits were successfully recovered in core samples on the landward side of the active foredune (Fig. 2). A trench of 2.5 m deep and 4 m long was excavated perpendicular to the trend of the beach ridge across the middle part of transect B, about 1160 m from the active coastline. This trench represents the sedimentary sequence and internal structures of the beach ridge. Based on lithology, stratigraphy and sedimentary structures, three distinct sedimentary units were identified (Fig. 3).

The upper unit is composed of yellowish, well-sorted fine to medium sand with large scale cross structures, plant roots and animal burrows. The thickness of the upper unit varies from 20 cm to more than 2 m in different cores. Under the microscope, sand grains appeared rounded to sub-rounded and were composed of eroded shell fragments,

foraminifer tests and siliciclastic components. This unit is identified as aeolian deposits. The aeolian sand terminates downward to coarse sand and gravel-size sediments with a sharp boundary. The middle unit is 2–4 m thick and mainly composed of biogenic carbonate, including marine shell fragments and foraminifer tests. This unit is composed of more than 70% carbonate with siliciclastic sand as a minor component. Upward fining of the grain size distribution and seaward dipping of large-scale cross-structures are characterizing the unit. The middle unit represents foreshore and upper foreshore deposits. Grain size and sediment composition of the unit is very similar to modern beach sediments (Table 1). The lower sedimentary unit is separated from the middle unit with a gradual boundary. It consists of green-gray, silty sand with scattered marine shells and shell fragments. Grain sizes are mainly in fine sand range and the carbonate content is 60–70%. The lower unit represents the lower shoreface sedimentary environment.

4.3. Ground penetrating radar profiles

The GPR profiles provide an insight to internal architecture of Chabahar strandplain. Transect B is selected as representative due to better data quality. Reflectors with similar properties such as shape, dip and termination type were grouped as radar units (Fig. 4). Supported by equivalent sedimentary units from sediment cores and trenches, radar units could be interpreted as equivalent to sedimentary facies. Three distinct radar units are identified in GPR profiles and named RF1, RF2 and RF3 respectively from the top to bottom (Table 2; Fig. 4). RF1 is characterized by parallel or gently landward dipping reflectors, with variable thickness and onlap or downlap termination to deeper reflectors. This radar unit is equivalent to aeolian deposits in sediment cores. RF2 is characterized by sigmoidal seaward dipping reflectors with overall upward convex shape mostly in toplap termination to the top and downlap contact to underlying reflectors. RF2 is equivalent to the foreshore and upper shoreface deposits.

RF3 consists of the deepest reflectors in the GPR profiles and is characterized by parallel to sub-parallel reflections. The middle unit (RF2) terminates to this unit with a downlap contact. RF3 is equivalent to the lower shoreface deposits of core and trench profiles.

4.4. Chronology of Chabahar strandplain

The chronology of Chabahar strandplain has established by radiocarbon dates of eight well-preserved marine mollusk shells collected from foreshore and upper shoreface deposits along transect A. The results are presented in Table 3 and the position of collected dating samples is shown in Fig. 5. A dating from transect C and Three radiocarbon dates from a former study (Gharibreza and Motamed, 2006) on the middle part of the strandplain close to transect B are also included in Fig. 5.
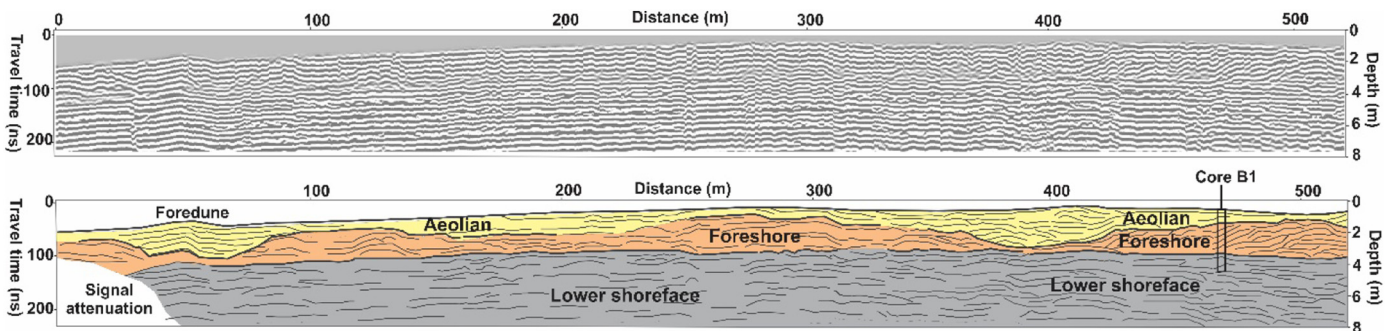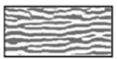

Fig. 4. Raw GPR profile (top) and its interpretation (bottom) from seaward section of transect B, radar facies are separated with colors and position of sediment core B1 is presented.

Table 2
Radar reflections patterns identified in GPR profiles and equivalent sedimentary facies.

Radar reflection pattern	Interpretation	Description	Radar facies	Sedimentary facies and environment
		Parallel or landward dipping reflectors, variable thickness, onlap or downlap termination	RF1	Aeolian sand
		Sigmoidal form, seaward dipping, overall convex upward, toplap termination to the top and downlap contact to underlying reflectors	RF2	Foreshore (beach) and upper shoreface
		Parallel to sub-parallel, downlap contact with upper unit	RF3	Lower shoreface

5. Discussion

5.1. Origin of Chabahar beach ridge system

Recent studies on beach ridge systems in various settings have revealed that diverse coastal processes are responsible for beach ridge formation (Hesp, 1984, 2006; Hesp et al., 2005; Otvos, 2000; Tamura, 2012). In prograding coasts, welding of coastal ridges and barriers is a commonly proposed mechanism. As sediments accumulate, bars and berms are isolated from the active shoreface and form relict shorelines (Stapor, 1975; Tanner, 1988; Tamura, 2012; Hein et al., 2013). Other mechanisms such as local oscillations in sea or lake level (Thompson and Baedke, 1995; Storms and Kroonenberg, 2007), aeolian processes (Taylor and Stone, 1996; Mauz et al., 2013) and periodic storms (Psuty, 1965; Storms and Kroonenberg, 2007; Nott et al., 2009) are also proposed for beach ridge formation. Under a relative sea-level fall regime, such as one across uplifting coasts, accommodation space migrates in the seaward direction, allowing the beach ridge system to prograde seaward in adequate sediment supply. Periodic variations in sediment input and accommodation space can explain the formation of ridge and swales at different elevations (Tanner, 1995; Otvos, 2000; Anthony, 2009). As it has demonstrated by Taylor and Stone (1996), a relative sea level fall cause wave base lowering and increase in sand availability on the costal shelf as the main source of sediment. In Chabahar Bay, marine biogenic carbonate is the major (70–80%) component of both modern beach and foreshore deposits across the beach ridges (Table 1). Sediment collected from beaches and upper shoreface is primarily composed of marine mollusk shells, shell fragments and foraminifera tests (Table 1; Fig. 2). The sedimentology and internal structure of beach ridges suggest that relict foreshore and upper shoreface deposits are originally formed in sedimentary environment equivalent to modern beach and shallow marine shelf (Figs. 2; 3; 4). Therefore, Chabahar strandplain is mainly composed of marine sediment and has formed by marine processes in normal energy conditions. Coastal plains have the potential to archive deposits from high energy waves such as severe storm and tsunamis (Atwater et al., 2012; May et al., 2012). Coastal boulders related to exceptionally large waves are found close to the study area (Shah-Hosseini et al., 2011). Further sedimentological and stratigraphic studies may reveal evidences for impact of high energy wave in Chabahar strandplain.

5.2. Beach ridges and past sea level

Beach ridges are demonstrated to be good indicators of the past sea level (Otvos, 2000; Goy et al., 2003; Anthony, 2009; Tamura, 2012). On the modern shoreline of Chabahar Bay, aeolian sand generally develops above maximum swash zone and form foredunes (Fig. 1d; Fig. 2). The capping sand on relict beach deposits introduce uncertainties in identifying the relationship between strandplain topography and sea level at the time of formation (Otvos, 1995, 1999, 2001; Tamura et al., 2008, 2010; Tamura, 2012) (Fig. 6). In order to reconstruct past sea levels, indicators that directly reflect wave processes are more accurate than beach ridge's surface. (Murray-Wallace et al., 1999; Otvos, 2000; Tamura et al., 2010; Tamura, 2012). The boundary between aeolian sand (foredune) and underlying foreshore (beach) facies is considered as a reliable sea level indicator. This boundary forms immediately above the level of landward swash limit of constructive waves (Van Heteren et al., 2000; Giosan et al., 2006; Rodriguez and Meyer, 2006) (Fig. 6). In the Chabahar strandplain, beach facies is generally characterized by coarse sand and abundant shells with seaward-dipping cross structures (Figs. 2; 3). Whereas fine to medium size aeolian sand exhibit gentle landward dipping cross beddings. Sharp sedimentological boundary between foreshore and aeolian facies is evident in core sediments as well as in GPR profiles (Table 2; Fig. 4). The tidal range is a major control on the position of the foreshore and foredune boundary. Today in Chabahar Bay, the sedimentological boundary between beach and foredune sediments is situated about 1 m above the mean sea level (Fig. 6). Assuming similar tidal range and wave conditions during formation of Chabahar strandplain, sea level stand is considered to be 1 m below the boundary of the beach and foredune deposits (Fig. 6; Fig. 7).

5.3. Reconstruction of Holocene relative sea level changes

Eight radiocarbon ages of marine shells collected from foreshore deposits along transect A are presented in Table 3, spatial distribution of ages is demonstrated in Fig. 5. As it debated above, the mean sea level was stand 1 m below foredune-beach boundary at the time of formation of the beach accretion (Fig. 6). Calibrated ages are plotted against the elevation of the aeolian-beach boundary for each sample (Fig. 7). This chronological model allows for reconstruction of relative sea level changes during formation of Chabahar strandplain. The beach ridge
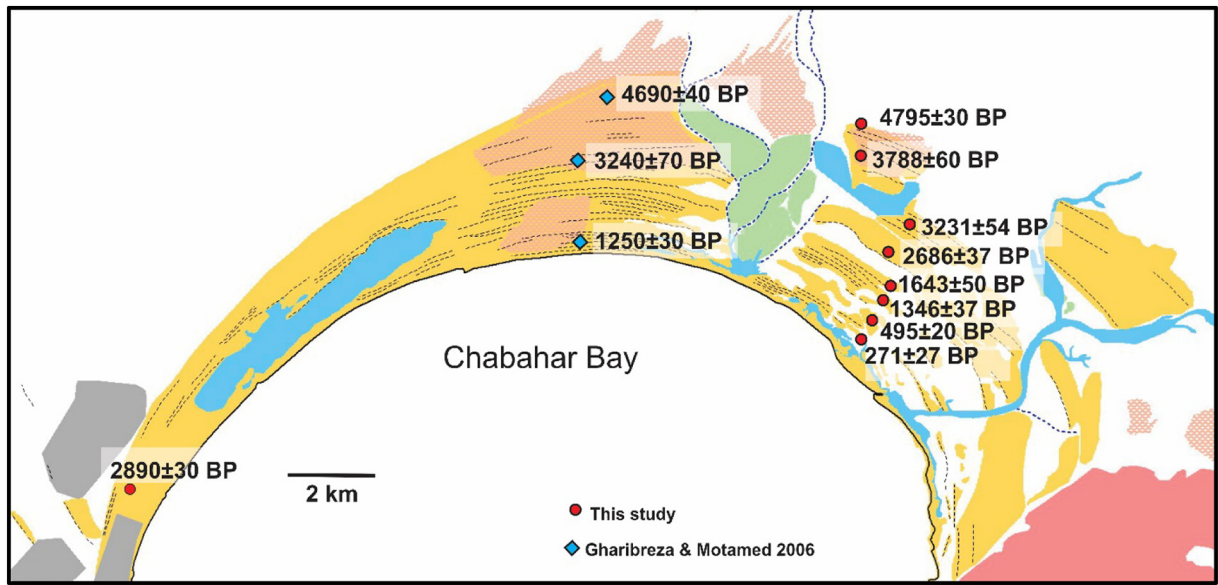
Table 3
Radiocarbon and calibrated ages of marine shells from foreshore and upper shoreface sediments of 8 beach ridges along transect A.

Sample Name	Mollusk family	Distance from modern shoreline (m)	Elevation from mean sea level (m)	C14 age	Calibrated age (2σ range)
R01	*Buccinidae*	4850	15.2	4555 ± 35	4795 ± 30 BP
R02	*Buccinidae*	4650	12.5	3840 ± 35	3788 ± 60 BP
R03	*Naticidae*	3550	8.5	3355 ± 30	3231 ± 54 BP
R04	*Tellinidae*	2950	7	2885 ± 30	2686 ± 37 BP
R05	*Olividae*	2450	6.5	2070 ± 30	1643 ± 50 BP
R06	*Olividae*	2000	5.2	1815 ± 30	1346 ± 37 BP
R07	*Architectonicidae*	1132	4	875 ± 25	495 ± 20 BP
R08	*Naticidae*	680	2	620 ± 30	271 ± 27 BP

Fig. 5. Calibrated radiocarbon ages for beach deposits from this study and former studies.
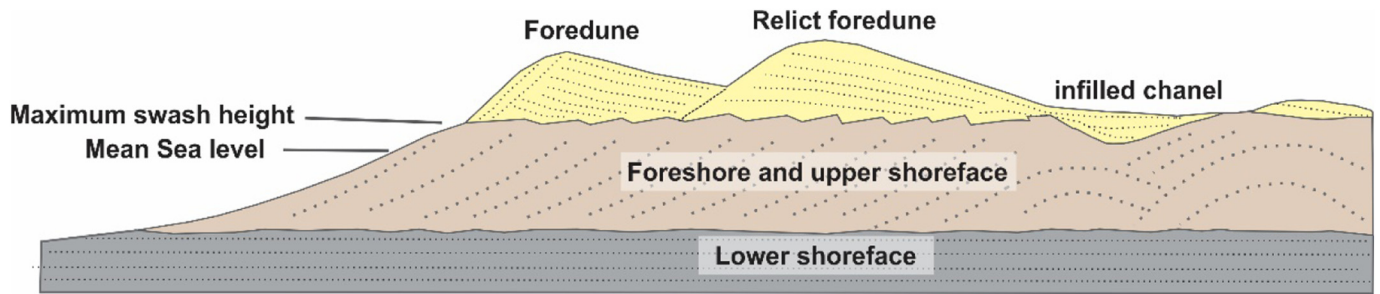

Fig. 6. Relation between mean sea level and maximum swash height with sedimentary facies in Chabahar strandplain.

system began to prograde after mid-Holocene sea level maximum around 4800 years before present. The youngest beach ridge has been isolated from the shoreline about 270 years before and situated in a distance of about 670 m from the modern shoreline (Fig. 1c). The evidence presented here point to a relative sea level fall of up to 15 m and

shoreline progradation of more than 5 km since last 4800 years (Fig. 7). The rate of relative sea level fall is approximately 3 mm/y along transect A in the eastern part of Chabahar strandplain (Fig. 1c; d). Based on radiocarbon dating of paleoshorelines by Gharibreza and Motamed (2006) (Fig. 5), the rate of relative sea level fall reaches up to 2.5 mm/y in the middle part of Chabahar strandplain (Fig. 1c; d). Only one dating has obtained from the western part of the Chabahar strandplain (Fig. 5), which suggest an approximated relative sea level fall of about 1.4 mm/y for this section of the coast (Fig. 1c; d).
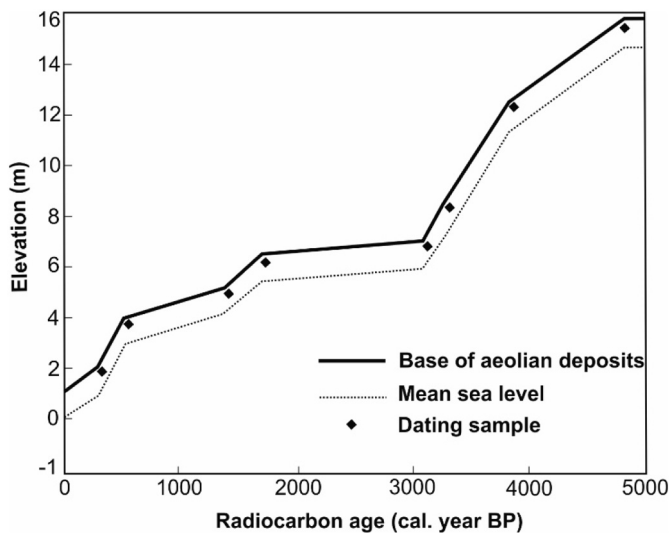
5.4. Relative sea level changes and active tectonics

The eustatic variations in sea level changes across the Makran coastal zone is not considerable since mid-Holocene (Reyss et al., 1998, Burg et al., 2012). Therefore, the relative sea level fall presented in Fig. 7 is reasonably attributed to the tectonic uplift of the coast. Coastal uplift in Iranian Makran have been estimated based on study of marine terraces in few former studies (Vita-Finzi, 1982, 1987, Reyss et al., 1998, Hosseini-Barzi and Talbot, 2003, Burg et al., 2012). Radiocarbon and uranium series datings on marine organisms collected from raised beaches west of Chabahar Bay yield an average Holocene uplift rate of 2 mm/y (Page et al., 1979; Reyss et al., 1998). In coastal Makran, uplift rates are mainly controlled by local geological structures. Mapping active faults shows that the Chabahar Bay is constrained by a conjugate set of faults (Hosseini-Barzi and Talbot, 2003). This section of the coast likely behaves as a fault-bounded block (Fig. 1c). Differential uplift in the eastern and western parts of the strandplain may be related to

Fig. 7. Radiocarbon ages plotted against elevation of beach-aeolian boundary and mean sea level for transect A.

different movement rates of bounding faults. However further study is needed for a detailed reconstruction of the coastal uplift history.

6. Conclusions

A vast strandplain around Chabahar Bay in SE Iran was studied using satellite imagery, digital elevation modelling, sedimentary analysis and ground penetrating radar. Subsurface profiles along with core and outcrop sedimentology provide insight into internal architecture of the strandplain. Sedimentology and fossil content suggest a principally marine origin for Chabahar strandplain. The boundary between aeolian and beach deposits indicates the position of former sea level, which is readily recognizable in sediment cores and GPR profiles. The chronology of the strandplain was established based on 9 radiocarbon dating on marine shells from beach sediments. The results show that the shoreline has prograded more than 5 km since the mid-Holocene (about 4800 year BP), and has been uplifted by up to 15 m in the eastern part of the strandplain. This relative sea level fall is attributed to tectonic uplift of the Makran coast. A gradual decrease in elevation of paleoshorelines from west to east indicates variations in relative sea level change most likely occurred due to different rates of tectonic uplift across the region.

Acknowledgment

References

Anthony, E.J., 1995. Beach-ridge development and sediment supply: examples from West Africa. Mar. Geol. 129, 175–186.

Anthony, E.J., 2009. Shore Processes and Their Palaeoenvironmental Applications. Developments in Marine Geology No. 4. Elsevier, Amsterdam (519 pp).

Atwater, B.F., ten Brink, U.S., Buckley, M., Halley, R.S., Jaffe, B.E., López-Venegas, A.M., Reinhardt, E.G., Tuttle, M.P., Watt, S., Wei, Y., 2012. Geomorphic and stratigraphic evidence for an unusual tsunami or storm a few centuries ago at Anegada, British Virgin Islands. Nat. Hazards 63, 51–84.

Billy, J., Robin, N., Hein, C.J., Certain, R., FitzGerald, D.M., 2014. Internal architecture of mixed sandand-gravel beach ridges: Miquelon-Langlade Barrier, NW Atlantic. Mar. Geol. 357, 53–71.

Billy, J., Robin, N., Hein, C.J., Certain, R., FitzGerald, D.M., 2015. Insight into the late Holocene Sea-level changes in the NW Atlantic from a paraglacial beach-ridge plain south of Newfoundland. Geomorphology 248, 134–146.

Blum, M.D., Sivers, A.E., Zayac, T., Goble, R.J., 2003. Middle Holocene sea-level and evolution of the Gulf of Mexico coast. Trans. Gulf Coast Assoc. Geol. Soc. 53, 64–77.

Bristow, C.S., Pucillo, K., 2006. Quantifying rates of coastal progradation from sediment volume using GPR and OSL: the Holocene fill of Guichen Bay, south-East South Australia. Sedimentology 53, 769–788.

Brückner, H., Schellmann, G., 2003. Late Pleistocene and Holocene shorelines of Andréeland, Spitsbergen (Svalbard): geomorphological evidence and palaeo-oceanographic significance. J. Coast. Res. 19, 971–982.

Burg, J.P., Dolati, A., Bernoulli, D., Smit, J., 2012. Structural style of the Makran Tertiary accretionary complex in SE Iran. In: Al Hosani, K., Roure, F., Ellison, R., Stephen, L (Eds.), Lithosphere Dynamics and Sedimentary Basins: The Arabian Plate and Analogues. Frontiers in Earth Sciences. Springer Verlag, Berlin Heidelberg, pp. 239–259.

Byrne, D.E., Sykes, L.R., Davis, D.M., 1992. Great thrust earthquakes and aseismic slip along the plate boundary of the Makran Subduction Zone. J. Geophys. Res. 97, 449–478.

Church, J.A., Clark, P.U., Cazenave, A., Gregory, J.M., Jevrejeva, S., Levermann, A., Merrifield, M.A., Milne, G.A., Nerem, R.S., Nunn, P.D., Payne, A.J., Pfeffer, W.T., Stammer, D., Unnikrishnan, A.S., 2013. Sea level change. In: Stocker, T.F., Qin, D., Plattner, G.-K., Tignor, M., Allen, S.K., Boschung, J., Nauels, A., Xia, Y., Bex, V., Midgley, P.M. (Eds.), Climate Change 2013: The Physical Science Basis. Contribution of Working Group I to the Fifth Assessment Report of the Intergovernmental Panel on Climate Change. Cambridge University Press, Cambridge, United Kingdom and New York, NY, USA.

Clemmensen, L.B., Nielsen, L., 2010. Internal architecture of a raised beach ridge system (Anholt, Denmark) resolved by ground-penetrating radar investigations. Sediment. Geol. 223, 281–290.

Gharibreza, M.R., 2016. Evolutionary trend of paleoshorelines in the coastal Makran zone (Southeast Iran) since the mid-Holocene. Quat. Int. 392, 203–212.

Gharibreza, M.R., Motamed, A., 2006. Late Quaternary paleoshorelines and sedimentary sequences in Chabahar Bay (Southeast of Iran). J. Coast. Res. 22 (6), 1499–1504.

Giosan, L., Donnelly, J.P., Constantinescu, S., Filip, F., Ovejanu, I., Vespremeanu-Stroe, A., Vespremeanu, E., Duller, G.A.T., 2006. Young Danube delta documents stable Black Sea level since the middle Holocene: morphodynamics, paleogeographic, and archaeological implications. Geology 34, 757–760.

Goy, J.L., Zazo, C., Dabrio, C.J., 2003. A beach-ridge progradation complex reflecting periodical sea-level and climate variability during the Holocene (Gulf of Almería, Western Mediterranean). Geomorphology 50, 251–268.

Hein, C.J., FitzGerald, D.M., Cleary, W.J., Albernaz, M.B., De Menezes, J.T., Klein, A.H.D.F., 2013. Evidence for a transgressive barrier within a regressive strandplain system: implications for complex coastal response to environmental change. Sedimentology 60, 469–502.

Hesp, P.A., 1984. Foredune formation in southeast Australia. In: Thom, B.G. (Ed.), Coastal Geomorphology in Australia. Academic Press, London, pp. 69–97.

Hesp, P.A., 2006. Sand beach ridges: definitions and re-definition. J. Coast. Res. Spec. Issue 39, 72–75.

Hesp, P.A., Dillenburg, S.R., Barboza, E.G., Tomazelli, L.J., Ayup-Zouain, R.N., Esteves, L.S., Gruber, N.L.S., Toldo Jr., E.E., De A. Tabajara, L.L.C., Clerot, L.C.P., 2005. Beach ridges, foredunes or transgressive dunefields? Definitions and an e amination of the Torres to Tramandai barrier system, southern Brazil. Ann. Braz. Acad. Sci. 77, 493–508.

Hosseini-Barzi, M., Talbot, C., 2003. A tectonic pulse in the Makran accretionary prism recorded in Iranian coastal sediments. J. Geol. Soc. 160, 903–910.

Jol, H.M., Lawton, D.C., Smith, D.G., 2002. Ground penetrating radar: 2-D and 3-D subsurface imaging of a coastal barrier spit, Long Beach, WA, USA. Geomorphology 53, 165–181.

Mauz, B., Hijma, M.P., Amorosi, A., Porat, N., Galili, E., Bloemendal, J., 2013. Aeolian beach ridges and their significance for climate and sea level: concept and insight from the Levant coast (East Mediterranean). Earth Sci. Rev. 121, 31–54.

May, S.M., Vött, A., Brückner, H., Grapmayer, R., Handl, M., et al., 2012. The Lefkada barrier and beachrock system (NW Greece) – controls on coastal evolution and the significance of extreme wave events. Geomorphology 139-140, 330–347.

McCall, G.J.H., Morgan, K.H., Campe, G.C., et al., 1985. Minab Quadrangle Map 1:250,000 and Explanatory Text. Geological Survey of Iran, p. 534.

McSaveney, M.J., Graham, I.J., Begg, J.G., Beu, A.G., Hull, A.G., Kim, K., Zondervan, A., 2006. Late Holocene uplift of beach ridges at Turakirae Head, south Wellington coast, New Zealand. N. Z. J. Geol. Geophys. 49 (3), 337–358.

Moore, L.J., Jol, H.M., Kruse, S., Vanderburgh, S., Kaminsky, G.M., 2004. Annual layers revealed by GPR in the subsurface of a prograding coastal barrier, southwest Washington, U.S.A. J. Sediment. Res. 74, 690–696.

Murray-Wallace, C.V., Belperio, A.P., Bouman, R.P., Cann, J.H., Price, D.M., 1999. Facies architecture of a last interglacial barrier: a model for Quaternary barrier development from the Coorong to Mount Gambier Coastal Plain, Southeastern Australia. Mar. Geol. 158, 177–195.

Nott, J., Smithers, S., Walsh, K., Rhodes, E., 2009. Sand beach ridges record 6000 year history of extreme tropical cyclone activity in northeastern Australia. Quat. Sci. Rev. 28, 1511–1520.

Oliver, T.S.N., Donaldson, P., Sharples, C., Roach, M., Woodroffe, C.D., 2017. Punctuated progradation of the Seven Mile Beach Holocene barrier system, southeastern Tasmania. Mar. Geol. 386, 76–87.

Otvos, E.G., 1995. Multiple Pliocene-Quaternary marine high stands, northeast Gulf coastal plain-fallacies and facts. J. Coast. Res. 11, 984–1002.

Otvos, E.G., 1999. Sediment and geomorphic criteria for reconstructing sea-level position, multiple Pliocene-Quaternary marine high stands on the northeastern Gulf of Mexico coastal plain. J. Coast. Res. 15, 1181–1187.

Otvos, E.G., 2000. Beach Ridges, Definitions and Significance. Geomorphology 32, 83–108.

Otvos, E.G., 2001. Assumed Holocene highstands, Gulf of Mexico: basic issues of sedimentary and landform criteria discussion. J. Sediment. Res. 71, 645–647.

Page, W.D., Alt, J.N., Cluff, L.S., Plafker, G., 1979. Evidence for the recurrence of large-magnitude earthquakes along the Makran Coast of Iran and Pakistan. Tectonophysics 52, 533–547.

Prins, M.A., Postma, G., Weltje, G.J., 2000. Controls on terrigenous sediment supply to the Arabian Sea during the late Quaternary: the Makran continental slope. Mar. Geol. 169, 351–371.

Psuty, N.P., 1965. Beach ridge development in Tabasco, Mexico. Ann. Assoc. Am. Geogr. 55, 112–124.

Regard, V., Bellier, O., Thomas, J.C., Bourlès, D., Bonnet, S., Abbassi, M.R., Braucher, R., Mercier, J., Shabanian, E., Soleymani, Sh., Feghhi, Kh., 2005. Cumulative right-lateral fault slip rate across the Zagros–Makran transfer zone: role of the Minab–Zendan fault system in accommodating Arabia–Eurasia convergence in southeast Iran. Geophys. J. Int. 162, 177–203.

Reimer, P.J., Bard, E., Bayliss, A., et al., 2013. IntCal13 and Marine13 radiocarbon age calibration curves 0–50,000 years cal BP. Radiocarbon 55 (4), 1869–1887.

Reyss, J.L., Pirazzoli, P.A., Haghipour, A., 1998. Quaternary marine terraces and tectonic uplift rates on the south coast of Iran. In: Stewart, I.S., Vita-Finzi, C. (Eds.), Coastal Tectonics. 146. Geological Society, London, Special Publications, pp. 225–237.

Rodriguez, A.B., Meyer, C.T., 2006. Sea-level variation during the Holocene deduced from the morphologic and stratigraphic evolution of Morgan Peninsula, Alabama, U.S.A. J. Sediment. Res. 76 (2), 257–269.

Scheffers, A., Engel, M., Scheffers, S., Squire, P., Kelletat, D., 2012. Beach ridge systems, archives for Holocene coastal events? Prog. Phys. Geogr. 36, 5–37.

Searle, D.J., Woods, P.J., 1986. Detailed documentation of a Holocene sea-level record in the Perth region, southern Western Australia. Quat. Res. 26, 299–308.

Shah-Hosseini, M., Morhange, C., Naderi Beni, A., Marriner, N., Lahijani, H., Hamzeh, M., Sabatier, F., 2011. Coastal boulders as evidence for high-energy waves on the Iranian coast of Makran. Mar. Geol. 290, 17–28.

Snead, R.E., 1970. Physical Geography of the Makran Coastal Plain of Iran. Rep. Off. Nav. Res., Contract N00014 66 C D104, Task Order NR388 082. University of New Mexico, Albuquerque (715pp).

Southon, J., Kashgarian, M., Fontugne, M., Metivier, B., Yim, W., 2002. Marine reservoir corrections for the Indian Ocean and Southeast Asia. Radiocarbon 44, 167–180.

Stapor, F.W., 1975. Holocene Beach-ridge Plain Development. 22. Zeitschrift für Geomorphologie, Northwest Florida, pp. 116–141 Supplementary Issue.

Storms, J.E.A., Kroonenberg, S.B., 2007. The impact of rapid sea level changes on recent Azerbaijan beach ridges. J. Coast. Res. 23 (2), 521–527.

Tamura, T., 2012. Beach ridges and prograded beach deposits as palaeoenvironment records. Earth Sci. Rev. 114, 279–297.

Tamura, T., Murakami, F., Nanayama, F., Watanabe, K., Saito, Y., 2008. Ground-penetrating radar profiles of Holocene raised-beach deposits in the Kujukuri strand plain, Pacific coast of eastern Japan. Mar. Geol. 248, 11–27.

Tamura, T., Murakami, F., Watanabe, K., 2010. Holocene beach deposits for assessing coastal uplift of the northeastern Boso Peninsula, Pacific coast of Japan. Quat. Res. 74, 227–234.

Tamura, T., Nicholas, W.A., Oliver, T.S.N., Brooke, B.P., 2017. Coarse-sand beach ridges at Cowley Beach, north-eastern Australia: their formative processes and potential as records of tropical cyclone history. Sedimentology. https://doi.org/10.1111/sed.12402.

Tanner, W.F., 1988. Beach ridge data and sea level history from the Americas. J. Coast. Res. 4, 81–91.

Tanner, W.F., 1995. Origin of beach ridges and swales. Mar. Geol. 129, 149–161.

Taylor, M., Stone, G.W., 1996. Beach-ridges: a review. J. Coast. Res. 12 (3), 612–621.

Thompson, T.A., 1992. Beach ridges development and lake-level variation in southern Lake Michigan. Sediment. Geol. 80, 305–318.

Thompson, T.A., Baedke, S.J., 1995. Beach-ridge development in Lake Michigan: shoreline behavior in response to quasi-periodic lake-level events. Mar. Geol. 129, 163–174.

Van Heteren, S., Huntley, D.J., van de Plassche, O., Lubberts, R.K., 2000. Optical dating of dune sand for the study of sea-level change. Geology 28, 411–414.

Vita-Finzi, C., 1982. Recent coastal deformation near the Strait of Hormuz. Proc. R. Soc. 382, 44–457.

Vita-Finzi, C., 1987. 14C deformation chronologies in coastal Iran, Greece and Jordan. J. Geol. Soc. Lond. 144, 553–560.